ELSEVIER

Thermochimica Acta 384 (2002) 291–301

thermochimica acta

www.elsevier.com/locate/tca

HMX decomposition model to characterize thermal damage

Michael L. Hobbs*

Sandia National Laboratories, Engineering Science Center, P.O. Box 5800, MS-0834, Albuquerque, NM 87185, USA

Abstract

Thermal decomposition of the crystalline explosive, octahydro-1,3,5,7-tetranitro-1,3,5,7-tetrazocine (HMX), is modeled using percolation theory in order to characterize thermal damage. Percolation theory has been used historically to describe fluid flow through a network of permeable and impermeable sites. To describe thermal decomposition, the permeable and impermeable sites are related to broken or unbroken bonds. For HMX, N_2O groups are treated as sites connected by oxygen and methyl bridges. Bridges connect the N_2O sites by C–N bonds and by intermolecular attractions between N and O. The gas-phase reaction of N_2O with CH_2O is also included in the mechanism. Predictions are compared to time-to-explosion data. The state of the condensed material at ignition is characterized by finite HMX-fragments of various molecular weights.

Keywords: HMX; Decomposition; Percolation theory; Cookoff; Thermal damage

1. Introduction

Octahydro-1,3,5,7-tetranitro-1,3,5,7-tetrazocine (HMX) decomposes by competing reaction pathways to form various condensed and gas-phase intermediate and final products. Gas formation is related to the development of nonuniform porosity and high specific surface area prior to ignition in cookoff events. Such thermal damage, created by various chemical and physical processes, enhances shock sensitivity and favors self-supported accelerated burning. Following ignition, the subsequent level of violence depends on the competition between dynamic pressure build-up and stress release caused by loss of confinement. The present work is aimed at predicting the path-dependent extent of reaction of HMX, which is needed to determine porosity, permeability, and specific surface area at ignition. The porosity, permeability, and specific surface area of the HMX at ignition become the initial condition for subsequent dynamic analysis that is beyond the scope of this paper.

A commonly used HMX decomposition model applied to cookoff analysis is the three-step global mechanism developed at Lawrence Livermore National Laboratories (LLNL) by Tarver and co-workers [1–3] based on one-dimensional time-to-explosion (ODTX) experiments

$$A \rightarrow B \rightarrow 2C \rightarrow D. \quad (1)$$

The activation energy for the initial endothermic reaction was obtained from the weakly confined Henkin test; the activation energy of the second mildly exothermic reaction was reported to be consistent with intermediate confinement tests, and the activation energy of the final highly exothermic reaction was based on measured gas-phase kinetics. The number of moles and identity of gases produced by each of the global reaction steps in Eq. (1) were not reported. As such, the LLNL mechanism is essentially a heat release mechanism used to obtain the time to thermal

* Fax: +1-505-844-8251.
E-mail address: mlhobbs@sandia.gov (M.L. Hobbs).

0040-6031/02/$ – see front matter
PII: S0040-6031(01)00784-5

runaway, and cannot be used to characterize thermal damage.

In the current work, a reaction mechanism is formulated based on the structure of the HMX molecule and the intermolecular interactions using percolation theory. The quantity and identity of the evolving gases, as well as the characteristics of the HMX-fragments in the solid residue, are resolved based on an assumed reaction pathway. The HMX percolation (HPERC) model discussed in this paper is based on two fundamental aspects of thermal decomposition [4]: (1) a kinetic bond breaking mechanism and (2) lattice statistics to describe the evolving solid. The HPERC parameters include the Arrhenius kinetics controlling bond breaking, the initial bridge population, and the coordination number. Low molecular weight products are assumed to have sufficiently high vapor pressures to evolve as gases.

The following section describes the pseudo infinite structure for the HMX crystals. Section 3 presents the chemical mechanism used to describe the disruption of the intermolecular forces between the HMX molecules and subsequent breaking of covalent bonds. Section 4 presents a brief description of the lattice statistics using percolation theory. Section 5 discusses the method used to determine the HPERC model parameters and includes a comparison between predicted and measured time to ignition for 1.27 cm diameter spheres of HMX exposed to various isothermal boundary conditions. Some general remarks close the paper.

2. Percolation lattice structure for HMX

Four polymorphs or solid phases of HMX: β-HMX, α-HMX γ-HMX and δ-HMX have frequently been reported in the literature [5], although γ-HMX is actually a hydrate of HMX as shown by Main et al. [6]. The most stable polymorph at room temperature, β-HMX, has a density of 1.9 g/cm^3, and the most stable polymorph at high temperatures, δ-HMX, has a density of 1.8 g/cm^3 [7]. Transformation from β-HMX to δ-HMX involves a significant volume change (∼5.5%) with associated crystalline damage and increased surface area. The reactivity of HMX is further enhanced as the ''chair-like'' ring conformation of β-HMX changes to the ''boat-like'' conformation

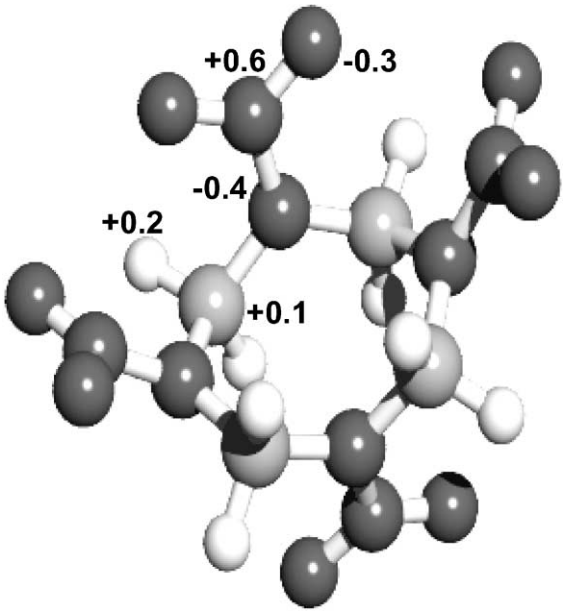

Fig. 1. Partial charges in β-HMX molecule.

of δ-HMX, since reactive >N–NO_2 side chains are in closer proximity to each other. Intermolecular forces need to be broken for HMX to change from the β- to the δ-polymorph of HMX. Thus, the initial step in HMX decomposition likely involves breaking of the intermolecular attractions between HMX molecules.

Fig. 1 shows an HMX molecule with partial charges labeled on some of the atoms determined with CHEM-3D [8] using an AM1 semi-empirical quantum mechanics calculation. The approximate charges on the outer nitrogen atoms are +0.6, and the approximate charges on the oxygen atoms are −0.3. Lewis et al. [9] postulate that HMX forms crystals primarily by electrostatic attraction between HMX molecules rather than hydrogen bonding. Because of the *strong intermolecular forces* between neighboring HMX molecules, each crystal of HMX can be thought of as being part of an infinite network.

Fig. 2A shows the basic building block of the essentially infinite HMX crystal structure. The N_2O group is considered the site for a real lattice with a coordination number, $\sigma + 1$, of 4. Fig. 2B shows an assumed lattice structure for HMX with four shaded building blocks comprising a single HMX molecule.

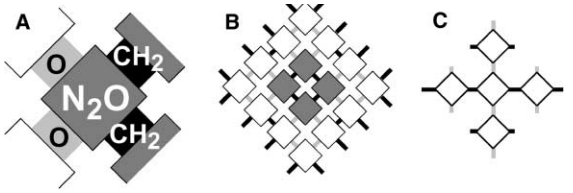

Fig. 2. (A) Basic building block, (B) real lattice, and C) pseudo Bethe lattice for HMX.

The lattice structure shown in Fig. 2B is considered a ''real'' lattice structure, since the lattice contains ''loop-backs'' where a path drawn from one site can eventually intersect the original site. Pseudo lattices, such as the tree-like Bethe lattice shown in Fig. 2C, do not contain ''loop-backs''. In the current paper, exact solutions to the lattice statistics are obtained by using Bethe lattice, which are shown in Fig. 2C.

Percolation theory has been used successfully to model polymer decomposition [4] by assuming the macromolecule is an infinite network of sites connected by bridges. For a smaller molecule, such as HMX, the infinite network is realized, since both bonds and intermolecular attractions connect the sites. In Fig. 2B, thick black lines represent bonds and gray lines represent intermolecular attractions. Fig. 2B shows eight possible intermolecular attractions per HMX molecule.

3. Kinetic mechanism

The basic building block of the HMX molecule shown in Fig. 2A consists of an N_2O site; oxygen bridges (Λ, labeled with an O in Fig. 2A); and methyl bridges (L, labeled with a CH_2 in Fig. 2A). The electrostatic attraction between an oxygen atom from one HMX molecule and the outer nitrogen atom in a neighboring HMX molecule forms an oxygen bridge, Λ. When the electrostatic attraction is broken, the oxygen does not connect the HMX molecules, and the oxygen bridge becomes an oxygen dangler, δ. Methyl bridges with the HMX ring, L, also connect N_2O sites. When the ring breaks, a methyl dangler, d, is formed. Fig. 3 further defines Λ, L, δ, and d.

The kinetic scheme, along with a graphical description of the HPERC decomposition mechanism, is shown in Fig. 3. Each of the bridges and danglers

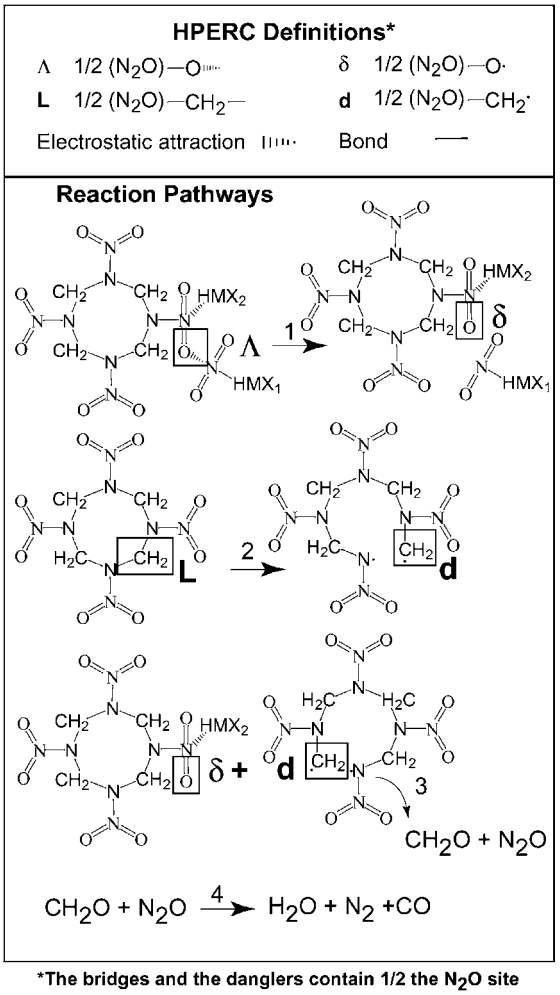

Fig. 3. HPERC definitions and reaction pathways.

are assumed to contain half of the N_2O site so that when an oxygen dangler reacts with a methyl dangler, N_2O and CH_2O are formed. The last step in the HPERC mechanism is the highly exothermic reaction of CH_2O and N_2O to form H_2O, N_2, and CO.

The reaction sequence begins when the intermolecular attractions between the HMX molecules are disrupted, and the oxygen bridges are broken. Without the intact oxygen bridges, the HMX is free to change from the ''chair'' configuration of β-HMX to the ''boat'' configuration of the δ-HMX polymorph. Another indication that the HMX molecule is free for solid–solid phase transformation is the condition

Table 1
HPERC mechanism, rate equations, and initial conditions

Reaction	Mechanism	Species	Rate equation	Initial condition
		Λ	$d\Lambda/dt = -k_1\Lambda$	$\Lambda\ (0) = \Lambda_0$
		L	$dL/dt = -k_2 L$	$L\ (0) = L_0$
(1)	$\Lambda \rightarrow \delta$	δ	$d\delta/dt = k_1\Lambda - k_3\delta d$	$\delta\ (0) = 0.5 - \Lambda_0$
(2)	$L \rightarrow d$	d	$dd/dt = k_2 L - k_3\delta d$	$d\ (0) = 0.5 - L_0$
(3)	$\delta + d \rightarrow N_2O + CH_2O$	N_2O	$dN_2O/dt = k_3\delta d - k_4[N_2O][CH_2O]$	$N_2O\ (0) = 0$
(4)	$N_2O + CH_2O \rightarrow H_2O + N_2 + CO$	CH_2O	$dCH_2O/dt = k_3\delta d - k_4[N_2O][CH_2O]$	$CH_2O\ (0) = 0$
		H_2O	$dH_2O/dt = k_4[N_2O][CH_2O]$	$H_2O\ (0) = 0$
		N_2	$dN_2/dt = k_4[N_2O][CH_2O]$	$N_2\ (0) = 0$
		CO	$dCO/dt = k_4[N_2O][CH_2O]$	$CO\ (0) = 0$

known as the critical percolation point, which is discussed further in Section 4.

With HMX in the ''boat'' configuration, the oxygen danglers and the methyl danglers are free to interact. Fig. 3 shows the danglers reacting to form CH_2O and N_2O. The final reaction in the HPERC mechanism is the reaction of CH_2O and N_2O to form small molecular weight gases. This simple mechanism is used to show that percolation theory can be used to model thermal decomposition of a crystalline material. A more accurate mechanism based on experiments such as solid-state NMR [10] is needed for accurate quantitative cookoff analysis. Although simplified, the HPERC mechanism shown in Fig. 3 is sufficient to replicate ODTX data.

Table 1 gives the mechanism, rate equations, and initial conditions for the HPERC model. The general reaction rate, r_j, for the HPERC model bond-breaking scheme is described by

$$r_j = k_j(T)\prod_{i=1}^{9} N_i^{\mu_{ij}}, \quad j = 1, \ldots, 4, \tag{2}$$

where N_i represents both population parameters Λ, L, δ, d and species parameters N_2O, CH_2O, H_2O, N_2, and CO. The concentration exponent matrix is represented by μ_{ij}, which is given in Table 2. The expressions for the kinetic coefficients, $k_j(T)$, are given in an Arrhenius form

$$k_j(T) = A_j \exp\left(\frac{-E}{RT}\right), \tag{3}$$

where A_j (s^{-1}), E_j (cal/mol or J/mol), and R (1.987 or 8.314 J/mol K) are the pre-exponential factors, activation energies, and universal gas constant, respectively. The species rate of change is given by

$$\frac{dN_i}{dt} = \sum_{j=1}^{4} v_{ij} r_j, \quad i = 1, \ldots, 9, \tag{4}$$

where v_{ij} are the stoichiometric coefficients of the jth reaction as given in Table 2. The kinetic mechanism requires the Arrhenius parameters, A_j and E_j, to be supplied for each reaction.

The initial labile bridge populations (Λ_0 and L_0) and the initial dangler population (δ_0 and d_0) need to be

Table 2
μ_{ij} and v_{ij} matrices

	r_1	r_2	r_3	r_4
μ_{ij}				
Λ	1	0	0	0
L	0	1	0	0
δ	0	0	1	0
d	0	0	1	0
N_2O	0	0	0	1
CH_2O	0	0	0	1
H_2O	0	0	0	0
N_2	0	0	0	0
CO	0	0	0	0
v_{ij}				
$d\Lambda/dt$	−1	0	0	0
dL/dt	0	−1	0	0
$d\delta/dt$	+1	0	−1	0
dd/dt	0	+1	−1	0
dN_2O/dt	0	0	+1	−1
dCH_2O/dt	0	0	+1	−1
dH_2O/dt	0	0	0	+1
dN_2/dt	0	0	0	+1
dCO/dt	0	0	0	+1

specified with the sum of all the bridges and danglers equal to unity. Half of the possible bridges are oxygen bridges and the other half of the bridges are methyl bridges. Therefore, the sum of the oxygen bridges and danglers equals to 0.5, and the sum of the methyl bridges and danglers also equals to 0.5. In this paper, the number of intermolecular attractions per HMX molecule is assumed to be ~2, which is 25% of the possible intermolecular attractions per HMX molecule. Thus, the initial oxygen bridge population, Λ_0, was set to 0.1 (25% of 0.5), and the initial oxygen dangler, δ_0, population was set to 0.4. Furthermore, since the ring is typically intact at normal conditions, L_0 and d_0 should be 0.5 and 0.0, respectively. The initial value problem described by Eqs. (1)–(3) is solved using DEBDF, a variable-order, backward-difference, ordinary differential equation solver package [11].

4. Lattice statistics

Percolation theory using Bethe lattices is used to characterize the degraded HMX crystal with regard to the size and population of finite fragments. The population variables determined from the kinetic mechanism can be used to determine the fraction of sites that are connected by bridges. For example, the fraction of intact bridges, p, can be determined as follows:

$$p = \Lambda + L \tag{5}$$

The mass fraction of finite fragments produced from the thermally degrading HMX depends on the population of intact bridges, p, determined from the kinetic mechanism and the coordination number, $\sigma + 1$. The lattice statistics are independent of the type of bridges connecting sites, provided the bridges are distinguished as either broken or intact. Thus, percolation theory can be used with any kinetic mechanism, provided the population of broken bridges $(1 - p)$ or intact bridges (p) is determined [12]. As the number of broken bridges increases, the fraction of finite fragments increases relative to the fraction of sites belonging to the infinite network. The infinite network no longer exists below a critical bridge population of $1/\sigma$ as shown by Fischer and Essam [13]. A detailed formulation of percolation theory, as used in the present paper, is given by Hobbs et al. [14].

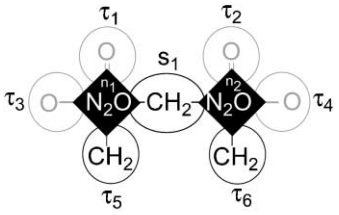

Fig. 4. Dimer (n-mer with two sites) showing σ, n, s, and τ.

For Bethe lattices, the number of finite fragments can be determined from the coordination number and the bridge population, p. The probability, F_n, that any given site is a member of a finite fragment of n-sites with s-bridges is

$$F_n = a_n p^s (1 - p)^\tau, \tag{6}$$

where

$$s = n - 1; \tag{7}$$

and

$$\tau = n(\sigma - 1) + 2 \tag{8}$$

where τ is the number of broken bridges on the perimeter of the HMX-fragment with s-bridges connecting n-sites as shown for the dimer in Fig. 4. The number of different ways to form such fragments is represented by a_n

$$a_n = \frac{\sigma + 1}{n\sigma + 1} \binom{n\sigma}{n - 1}, \tag{9}$$

where the binomial expression is

$$\binom{n\sigma}{n - 1} = \frac{(n\sigma + 1)!}{(n - 1)![n(\sigma - 1) + 2]!}. \tag{10}$$

Eq. (6) formally states that the probability that any given bridge belongs to an n-mer is the probability that the given bridge is intact or occupied (p^s) multiplied by the probability that the nearest neighbor bridges are broken or unoccupied $(1 - p)^\tau$ with a_n accounting for the distinct number of configurations possible for the n-mer. Eqs. (6)–(10) are discussed further in [12–14].

The mass fraction and molecular weight of each HMX-fragment bin can be determined by relating the

total mass and finite fragment mass on a site basis. A site is defined as the N_2O group shown in Fig. 4 including half the bridge mass. The rest of the bridge mass is associated with the neighboring sites. The total mass per site is

$$m_t = M_{N_2O} + \frac{M_b}{2}(\sigma + 1), \tag{11}$$

where M_{N_2O} is the molecular weight of N_2O as represented by the diamond in Fig. 4, $M_b/2$ half the molecular weight of the bridges connecting the N_2O groups, and $\sigma + 1$ the coordination number. For the HMX lattice, the coordination number is 4, and M_b is the average bridge molecular weight, $(M_{CH_2} + M_O)/2$. Thus, Eq. (11) becomes

$$m_t = M_{N_2O} + M_{CH_2} + M_O = 74\,\mathrm{g/mol}. \tag{12}$$

The mass of gas released can also be expressed on a site basis as

$$m_g = \left[\sum_{i=1}^{5} \frac{M_i N_i}{2}\right](\sigma + 1), \tag{13}$$

where M_i is the molecular weight of the ith gas, and N_i the population parameter described in Eq. (4). These weights are divided by two to normalize the gas populations to the total mass per site given in Eq. (11). Expansion of Eq. (13) gives

$$\begin{aligned} m_g = 2\{&M_{N_2O}[N_{N_2O}] + M_{CH_2O}[N_{CH_2O}] + M_{H_2O}[N_{H_2O}] \\ &+ M_{N_2}[N_{N_2}] + M_{CO}[N_{CO}]\}, \end{aligned} \tag{14}$$

where the progress of the individual gases (N_i) is given in square brackets. The mass of each gas, M_i, is 44, 30, 18, 28, and 28 g/mol for N_2O, CH_2O, H_2O, N_2, and CO, respectively.

The mass of a finite fragment expressed on a site basis, m_n, can be determined from the mass of the finite fragment, M_n, multiplied by the n-site fragment population on a site basis, Q_n

$$m_n = M_n Q_n, \tag{15}$$

where

$$\begin{aligned} M_n = {} & nM_{N_2O} + (n-1)M_\Lambda\left(\frac{\Lambda}{p}\right) + (n-1)(M_L)\left(\frac{L}{p}\right) \\ & + \frac{M_\delta}{2}\left[\frac{\tau\delta}{(1-p)}\right] + \frac{M_d}{2}\left[\frac{\tau d}{(1-p)}\right]; \end{aligned} \tag{16}$$

and

$$Q_n = \frac{F_n}{n} = \frac{[a_n p^{n-1}(1-p)^{n(\sigma-1)+2}]}{n}. \tag{17}$$

M_n is the molecular weight of the nth HMX-fragment bin. The first term in Eq. (16) represents the number of N_2O sites in the n-mer multiplied by the site molecular weight. The second term in Eq. (16) represents the number of bridges, $n-1$, in the HMX-fragment multiplied by the mass of the bridges of type Λ. The third term in Eq. (16) represents the number of bridges in the HMX-fragment multiplied by the mass of the bridges of type L. The last two terms in Eq. (16) represent the weight of the side-chains, or ''danglers'', which can evolve over time. The factors $\delta/(1-p)$ and $d/(1-p)$ represent the fraction of side-chains of type δ and d, respectively. The fraction of broken bridges with one side-chain being formed from each broken bridge is represented by $(1-p)$, and τ is the number of bridges that isolate a HMX-fragment as given in Eq. (8). The factor ''2'' in the denominator of the last two terms in Eq. (16) is needed to be consistent with the half bridge basis used in Eq. (11).

An explicit expression for Q_n can be obtained for HMX with a coordination number of 4 by combining Eqs. (9) and (17)

$$Q_n = \frac{4(3n)!}{n![2(n+1)]!} p^{n-1}(1-p)^{\tau}. \tag{18}$$

The term $4(3n)!/n![2(n+1)]!$ is 1, 2, and 6 for the HMX monomer, dimer, and trimer, respectively.

The primary variables of interest for the network statistical model are the mass fraction of the gas ($f_g = m_g/m_t$ where m_g is calculated from Eq. (14) and m_t is calculated from Eq. (12)), the solid fraction ($f_s = 1 - f_g$); the molecular weight of the nth HMX-fragment (M_n, Eq. (16)), and the mass fraction of the nth HMX-fragment ($f_n = m_n/m_t$, where m_n is calculated from Eq. (15)).

5. Parameters and data comparison

Tarver and co-workers [1–3] ODTX experimental database was used to obtain the kinetic parameters listed in Table 3. In the ODTX experiments, preheated aluminum anvils were machined in order to confine a

Table 3
Kinetic and thermal properties

$\ln A_1$[a]	32.4
$\ln A_2$	34.6
$\ln A_3$	41.4
$\ln A_4$	31.3
E_1/R[b](K)	20700
E_2/R (K)	20100
E_3/R (K)	23100
E_4/R (K)	17800
q_1[c] (cal/g)	−675
q_2 (cal/g)	−581
q_3 (cal/g)	+989
q_4 (cal/g)	+1,030
C_p[d] (20 °C)	0.24
C_p (350 °C)	0.42
λ[e] (20 °C)	0.00123
λ (160 °C)	0.00097
ρ (g/cm^3)	1.9
T_{melt} (°C)	247
Latent enthalpy (cal/g)	50

[a] $\ln A_i$ represents the natural logarithm of the frequency factor (s^{-1}) for reaction i.
[b] Activation energy divided by gas constant.
[c] Negative reaction enthalpies are endothermic.
[d] Heat capacity units are in cal/g K.
[e] Thermal conductivity units are in cal/cm s K.

1.27 cm diameter spherical sample of explosive using a copper-sealing ring [15]. The aluminum anvils were held together using a hydraulic press. The actual pressure within the spherical inclusion is not measured. Heaters were used to control the temperature of the anvils to ±0.2 °C, and the primary response is the acoustically measured time-to-explosion. The time-to-explosion can either be a thermal runaway (external temperature is above the critical temperature) or a pressure burst (external temperature is at or below the critical temperature). An overview of thermal initiation of explosives can be found in [16–18].

An explosive chemical kinetics code, XCHEM [19], was used to solve the reactive diffusion equations associated with thermal ignition of HMX using the HPERC reaction mechanism given previously in Table 1. This method-of-lines code uses stiff numerical methods and adaptive meshing to resolve relevant combustion physics. Solution accuracy is maintained between multilayered materials consisting of blends of reactive components and/or inert materials. Temperature-dependent thermal properties have been incorporated, and the modifications of thermal conductivities to include decomposition effects are estimated using solid/gas volume fractions determined by species fractions. Gas transport properties, including high-pressure corrections, have also been included, although these correlations are not used for the HMX calculations performed using HPERC. Time-varying temperature, heat flux, convective and thermal radiation boundary conditions, and layer-to-layer contact resistance have also been implemented into XCHEM.

Table 3 gives the mean values of the parameters used in the HPERC decomposition model. Table 3 also includes the thermophysical properties of the HMX used for the ODTX calculations. The temperature-dependent thermal conductivity and heat capacity were taken from [2]. The thermal conductivities were interpolated using a semi-log interpolation method.

The Arrhenius parameters in Table 3 were obtained by minimizing the error between the calculated and measured time-to-explosion for two external temperature boundary conditions, 280 and 227 °C

$$\text{error} = \frac{|t_{280}^{\text{HPERC}} - t_{280}^{\text{mea}}|}{t_{280}^{\text{mea}}} + \frac{|t_{227}^{\text{HPERC}} - t_{227}^{\text{mea}}|}{t_{227}^{\text{mea}}} \quad (19)$$

The measured time-to-explosion for these two temperatures (t_{227}^{mea} and t_{280}^{mea}) was taken to be 3 and 600 s, respectively. The DAKOTA tool-kit [20] which utilizes object-oriented design to interface analysis codes to various optimization techniques, was used to minimize the error in Eq. (19). Fig. 5 shows the conceptualized XCHEM interface with the Dakota tool-kit. The input deck generator was based on an algebraic preprocessor, APREPRO [21]. The error calculator, a FORTRAN code, was used to read XCHEM [19] output and compute the error function given in Eq. (19). A C-shell script controlled the input generator and error calculator.

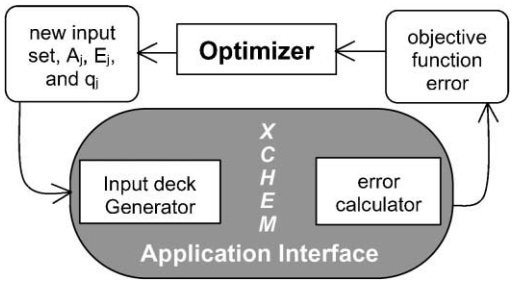

Fig. 5. XCHEM interface with DAKOTA.

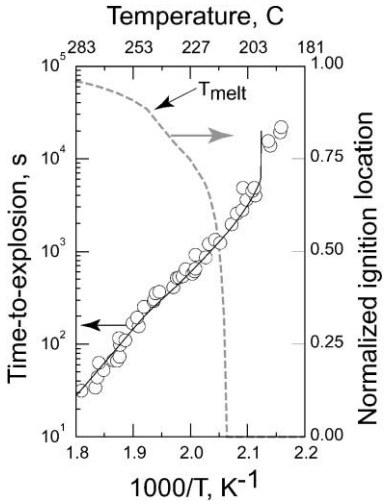

Fig. 6. Calculated (line) and experimental (circle) time-to-explosion for 1.27 cm diameter spheres of HMX.

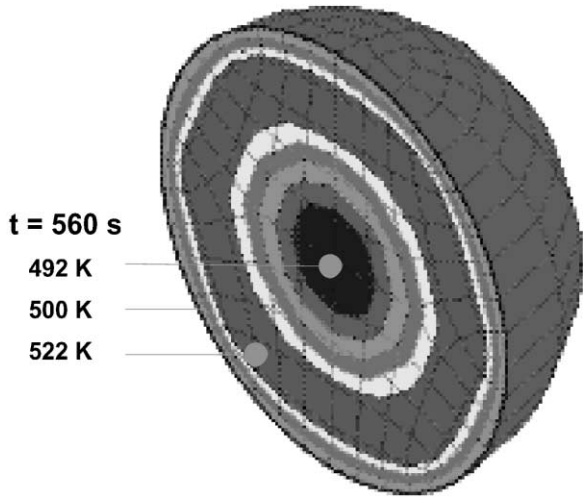

Fig. 7. Temperature near ignition.

Fig. 6 shows a plot of the logarithm of ignition time for HMX versus the ODTX anvil temperatures, T_a. In these plots, the logarithm of ignition time versus 1000/T_a is nearly linear over a large temperature range, but bends upward sharply near the critical temperature. The lines are XCHEM calculations using the HPERC mechanism, and the symbols correspond to experimental data from Tarver et al. [1].

The dashed line in Fig. 6 shows the normalized ignition location with the center of the HMX located at zero and the edge of the HMX located at one. Generally, ignition located near the heated boundary results in a lower intensity event because of early failure of the charge confinement. Ignition events located at the center of the charge often result in violent events that are enhanced by the uniformly heated, self-confined energetic material. Fig. 6 shows a change in slope in the normalized ignition location at the HMX melting temperature (247 °C, [7]). This slight change in slope is also apparent in the time-to-explosion data and calculations.

Fig. 6 also shows essentially a vertical line at the HPERC critical temperature of 198 °C, where energy is dissipated by conduction faster than energy is being generated by reactions. The experimental data points taken at temperatures below the predicted critical temperature might be a result of a pressure burst rather than a thermal runaway. A thermal, chemical, and mechanical calculation is needed to predict results below the critical temperature. Since the predictions in this paper only include thermal and chemical analysis, prediction of pressure burst below the critical temperature is beyond the scope of the current work. However, the interested reader can consult [22–26] for more information regarding coupled thermal, chemical, and quasi-static mechanical analysis.

Fig. 7 shows the temperature in a 1.27 cm diameter sphere of HMX exposed to a constant boundary temperature of 500 K. Radial profiles of temperature, solid fraction, average gas molecular weight, the bridge population, n-mer weight fractions, and n-mer molecular weight distributions are shown in Fig. 8. The profiles are taken near the ignition point, which occurs at approximately 10 min.

As shown in Fig. 7 and again in Fig. 8A, ignition occurs near the normalized radius, r/r_0, of 0.75. At this location, the temperature is starting to increase above the 500 K boundary temperature, which is maintained at the edge of the HMX sphere. In Fig. 8B the solid fraction is about 0.55 near the outer edge of the explosive. The integrated solid fraction can be determined for the entire sphere as follows:

$$\phi_f = \frac{4\pi \int_0^R r^2 f_s \, \mathrm{d}r}{(4/3)\pi R^3}, \tag{20}$$

where $f(r)$ is the solid fraction shown in Fig. 8B. The integrated solid fraction calculated from Eq. (20) is

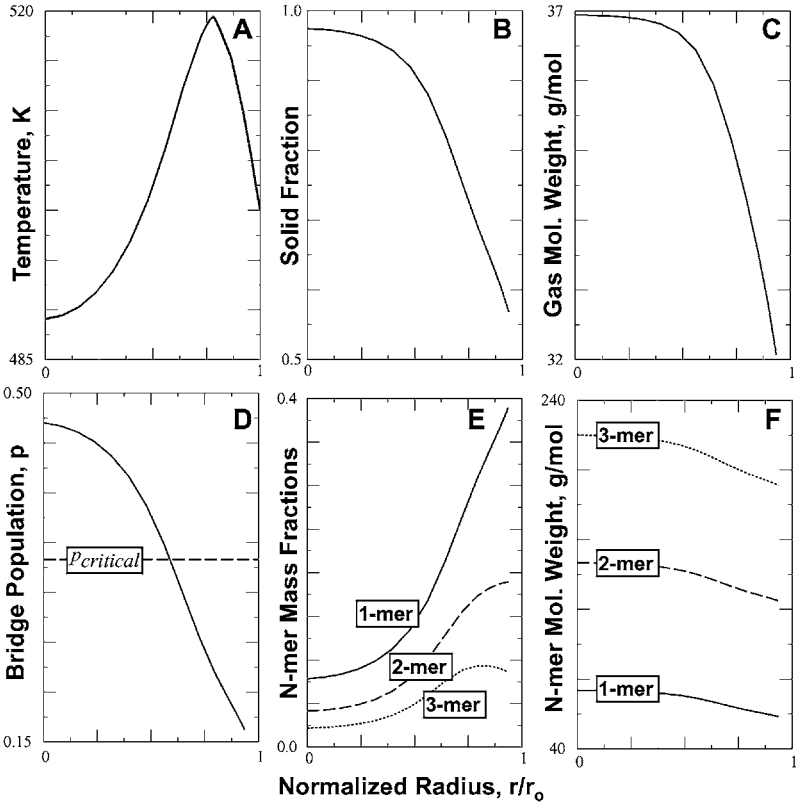

Fig. 8. HPERC calculated profiles of (A) temperature, (B) solid fraction, (C) gas molecular weight, (D) bridge population with the critical bridge population shown as a dashed line, (E) *n*-mer mass fraction, and (F) *n*-mer molecular weight. The calculation was performed on a 1.27 cm diameter sphere of HMX with a 500 K constant temperature boundary condition. The profiles are plotted just before thermal runaway that occurs after about 10 min. Input parameters are given in Table 3.

approximately 0.75, giving an overall reacted gas fraction of 0.25.

A conservative estimate of the ideal gas (36 g/mol) pressure at these conditions would be 550 bars (8000 psi)

$$P \approx 0.25(1.9\,\mathrm{g/cm^3})(500\,\mathrm{K}) \times (83.15\,\mathrm{cm^3\,bar/mol\,K})/(36\,\mathrm{g/mol}) = 550\,\mathrm{bars}. \quad (21)$$

This ideal gas pressure estimate is low since the volume of the unreacted solid was neglected. Nevertheless, at these high pressures, the confinement may pressure burst before thermal runaway is achieved. Experimental evidence is needed to determine whether the time-to-explosion corresponds to a thermal runaway or a pressure burst. The HPERC model can be fit to either thermal runaway data or pressure burst data. Without pressure measurements, the nature of the decomposition products is unknown. At high pressure in the ODTX experiment, the H_2O is almost certainly a compressed liquid, and the N_2O and CH_2O are likely supercritical fluids. More data is needed to predict the confined pressurization of decomposing HMX.

Fig. 8D shows the bridge population just before thermal runaway. The critical bridge population for the HMX lattice with a coordination number of 4 is $1/(4-1)$ or 1/3. This critical bridge population is labeled in Fig. 8D as p critical. When p is above the critical percolation point, an infinite lattice structure is maintained. Below the critical percolation point, only finite HMX-fragments exist. The critical percolation point may indicate when the molecule is free to undergo

the conformation change from the β- to δ-phase of HMX. The *n*-mer mass fractions and molecular weights are shown in Fig. 7E and F, respectively. A percolation theory-based model, such as the HPERC model, can give information regarding the evolving solid. The thermal damaged state of the HMX near cookoff conditions may be related to the HMX-fragment populations as characterized in Fig. 7E and F.

6. Future needs

The HPERC decomposition model, with the parameters given in Table 3, should only be applied to cookoff scenarios that are similar to the ODTX experiments. The mechanism and/or model parameters could be improved with data from well-characterized cookoff experiments. These cookoff experiments should be repeatable, gas leaks should either be eliminated or measured, pressure should be measured, and thermal/mechanical properties should be determined for pristine as well as degraded HMX. For example, significant differences in thermal/mechanical properties are expected with substantial density changes due to phase change and/or reaction. The properties for thermally degraded materials could then be related to micro-scale processes in order to give insight into appropriate mixture models.

Quantitative structure-activity relationships (QSAR) may also be used to quantitatively correlate evolving molecular structure, as determined with a model such as HPERC, to macroscale properties such as porosity, permeability, or specific surface area at ignition. QSAR techniques have been used in the pharmaceutical industry to determine reactivity and may be useful for cookoff analysis. QSAR descriptors such as solvent-accessible surface area may be related to specific surface area, which is necessary for post-ignition analysis.

7. Summary and conclusions

Percolation theory has been used to model HMX decomposition by identifying the basic structural unit of the HMX molecule. The HMX crystal was modeled as an infinite network of N_2O sites connected by methyl bridges and intermolecular attractions between oxygen and nitrogen in separate HMX molecules. Electrostatic potential charges for the outer nitrogen atoms were calculated using a semi-empirical quantum mechanics calculation. The charges on the outer nitrogen atoms were approximately $+0.6$, and the electrostatic potential charges on the oxygen atoms were approximately -0.3. A chemical structure-based model such as HPERC is necessary to predict evolving surface area and porosity to fully characterize thermal and chemical damage. The current paper describes only the changing chemical structures. More work is needed to relate the chemical structures to physical properties needed to predict violence.

A simple four-step mechanism was postulated for the breaking of the intermolecular attractions between the HMX molecules and cleavage of the HMX ring. A simple gas-phase reaction of N_2O with CH_2O to form small molecular weight gases completes the mechanism. The kinetic parameters for the bond-breaking scheme were determined by using an optimizer to minimize the error between the predicted and measured time-to-explosion in the ODTX experiment. The model was used to predict time-to-explosion with a reasonable degree of accuracy. Plots of the temperature profile just before ignition, the evolving solid fraction, average gas molecular weight, bridge population, and HMX-fragment populations were also presented. Prediction of pressure within the ODTX experimental apparatus was shown to be difficult without an appropriate equation-of-state for the decomposition products. More characterization of the ODTX experiment with a measurement of internal pressure and radial temperature profiles is needed. In addition, the relationship between the predicted HMX-fragments and physical properties such as surface area should be determined using techniques like QSAR to relate chemical structure information to reactivity.

Acknowledgements

This work performed at Sandia National Laboratories. Sandia is a multiprogram laboratory operated by Sandia Corporation, a Lockheed Martin Company, for the US Department of Energy under contract DE-ACO4-94AL85000. I gratefully acknowledge the many modeling discussions related to percolation

theory from D.M. Grant (University of Utah), R.J. Pugmire (University of Utah), and T.H. Fletcher (Brigham Young University). W.W. Erikson helped formulate the ideas related to inclusion of half the N_2O sites with the danglers. M.S. Eldred helped set-up the DAKOTA optimizer used to obtain the kinetic parameters. Comments from internal reviewers at Sandia National Laboratories, M.R. Baer, E.S. Hertel, and R.G. Schmitt, are also appreciated.

References

[1] C.M. Tarver, S.L. Chidester, A.L. Nichols Jr., J. Phys. Chem. 100 (1996) 5794.
[2] R.R. McGuire, C.M. Tarver, Chemical decomposition models for the thermal explosion of confined HMX, TATB, RDX, and TNT explosives, in: Proceedings of Seventh International Symposium on Detonation, NSWC MP 82–334, Naval Surface Weapons Center, White Oak, MA, 1981, p. 56.
[3] C.M. Tarver, R.R. McGuire, E.L. Lee, E.W. Wrenn, K.R. Brein, The thermal decomposition of explosives with full containment in one-dimensional geometries, in: Proceedings of Seventeenth International Symposium on Combustion, The Combustion Institute, Pittsburgh, PN, 1979, p. 1407.
[4] M.L. Hobbs, K.L. Erickson, T.Y. Chu, Polym. Degrad. Stabil. 69 (2000) 47.
[5] F. Goetz, T.B. Brill, J.R. Ferraro, J. Phys. Chem. 82 (1978) 1912.
[6] P. Main, R.E. Cobbledick, R.W.H. Small, Acta Cryst. 41 (1985) 1351.
[7] T.R. Gibbs, A. Popolato (Eds.), LASL Explosive Property Data, University of California Press, Berkeley, CA, 1980.
[8] CHEM3D Molecular Modeling and Analysis, Version 5, software from http://www.camsoft.com.
[9] J.P. Lewis, T.D. Sewell, R.B. Evans, G.A. Voth, J. Phys. Chem. B 104 (2000) 1009.
[10] M.S. Solum, R.J. Pugmire, D.M. Grant, Energy and Fuels 3 (1989) 187.
[11] L.F. Shampine, H.A. Watts, DEPAC-design of a user oriented package of ODE solvers, Sandia National Laboratories Report, SAND79-2374, Albuquerque, NM, 1979.
[12] D.M. Grant, R.J. Pugmire, T.H. Fletcher, A.R. Kerstein, Energy and Fuels 3 (1988) 175.
[13] M.E. Fisher, J.W. Essam, J. Math. Phys. 2 (1961) 609.
[14] M.L. Hobbs, K.L. Erickson, T.Y. Chu, Modeling decomposition of unconfined rigid polyurethane foam, Sandia National Laboratories Report, SAND99-2758, Albuquerque, NM, 1999.
[15] E. Catalano, R. McGuire, E. Lee, Wrenn D. Ornellas, J. Walton, The thermal decomposition and reaction of confined explosives, in: Proceedings of Sixth International Symposium on Detonation, ACR-221, Office of Naval Research, Department of the Navy, Arlington, VA, 1976, p. 214.
[16] J. Zinn, C. Mader, J. Appl. Phys. 31 (1960) 323.
[17] J. Zinn, R.N. Rogers, J. Phys. Chem. 66 (1962) 2646.
[18] A.G. Merzhavov, V.G. Abramov, Propellants and Explosives 6 (1981) 130.
[19] R.J. Gross, M.R. Baer, M.L. Hobbs, XCHEM-1D: A heat transfer/chemical kinetics computer program for multilayered reactive materials, Sandia National Laboratories Report SAND93-103, Albuquerque, NM, 1993.
[20] M.S. Eldred, Optimization strategies for complex engineering applications, Sandia National Laboratories Report, SAND98-034, Albuquerque, NM, 1998.
[21] G.D. Sjaardema, APREPRO: An algebraic preprocessor for parameterizing finite element analyses, Sandia National Laboratories Report, SAND92-2291, Albuquerque, NM, 1994.
[22] M.L. Hobbs, M.R. Baer, R.J. Gross, A constitutive mechanical model for cookoff of energetic materials, In: Proceedings of Twentieth International Pyrotechnics Seminar, Colorado Springs, CO, 1994, p. 423.
[23] R.J. Gross, M.R. Baer, M.L. Hobbs, Mechanical effects in cookoff modeling, in: Proceedings of Twentieth International Pyrotechnics Seminar, Colorado Springs, CO, 1994, p. 355.
[24] M.L. Hobbs, M.R. Baer, R.J. Gross, Thermal–chemical–mechanical cookoff modeling, in: Proceedings of JANNAF Propulsion Systems Hazards Subcommittee Meeting, CPIA publication 615, San Diego, CA, 1994, p. 311.
[25] M.L. Hobbs, M.R. Baer, Multidimensional fully-coupled thermal–chemical–mechanical response of reactive materials, in: Procedings of JANNAF Propulsion Systems Hazards Subcommittee Meeting, NASA Marshall Space Flight Center, Huntsville, AL, 1995.
[26] M.R. Baer, M.L. Hobbs, R.J. Gross, R.G. Schmitt, Cookoff of energetic materials, in: Proceedings of Eleventh International Symposium on Detonation, Snowmass, CO, 1998.